

Two forms of aftereffects induced by transparent motion reveal multilevel adaptation

Alan L. F. Lee

Department of Psychology, University of California,
Los Angeles, CA, USA



Department of Psychology, University of California,
Los Angeles, CA, USA, &

Department of Statistics, University of California,
Los Angeles, CA, USA



Hongjing Lu

Visual adaptation produces remarkable perceptual aftereffects. However, it remains unclear what basic neural mechanisms underlie visual adaptation and how these adaptation-induced neural changes are related to perceptual aftereffects. To address these questions, we examined transparent motion adaptation and traced the effects of adaptation through the motion processing hierarchy. We found that, after adapting to a bidirectional transparent motion display, observers perceived two radically different motion aftereffects (MAEs): segregated and integrated MAEs, depending on testing locations. The segregated MAE yielded an aftereffect opposite to one of the adapting directions in the transparent motion stimulus. Our results revealed that the segregated MAE relies on the integration of local adaptation effects. In contrast, the integrated MAE yielded an aftereffect opposite to the average of the adapting directions. We found that integrated MAE was dominant at non-adapted locations but was reduced when local adaptation effects were weakened. These results suggest that integrated MAE is elicited by a combination of two mechanisms: adaptation-induced changes at a high-level processing stage and integration of local adaptation effects. We conclude that distinct perceptual aftereffects can be observed due to adaptation-induced neural changes at different processing levels, supporting the general hypothesis of multilevel adaptation in the visual hierarchy.

Keywords: motion, adaptation, aftereffects, multilevel, transparent motion, processing hierarchy

Citation: Lee, A. L. F., & Lu, H. (2012). Two forms of aftereffects induced by transparent motion reveal multilevel adaptation. *Journal of Vision*, 12(4):3, 1–13, <http://www.journalofvision.org/content/12/4/3>, doi:10.1167/12.4.3.

Introduction

Previous neurophysiological studies have found that, after prolonged stimulation, neurons in the visual cortex change their response characteristics (Dragoi, Sharma, & Sur, 2000; Kohn & Movshon, 2003, 2004; Krelberg, van Wezel, & Albright, 2006) and that such adaptation-induced neural changes are related to remarkable perceptual aftereffects (Schrater & Simoncelli, 1998; Verstraten, Fredericksen, & van de Grind, 1994; for a review, see Clifford et al., 2007). The special case of contrast adaptation has been extensively studied over the past 20 years. Converging physiological and psychophysical evidence has shown that contrast adaptation induces neural changes through two mechanisms. First, adaptation independently modulates neural activity at early processing stages such as retina and V1 (Baccus & Meister, 2004; Solomon, Peirce, Dhruv, & Lennie, 2004); second, these low-level changes are propagated up the visual hierarchy to affect neural responses in higher level areas such as MT (Kohn & Movshon, 2003). It remains unclear whether these two basic mechanisms are also recruited for other types of sensory adaptation and whether adaptation-induced neural

changes at different processing levels can lead to distinct perceptual aftereffects. To address these questions, the present study investigates a different form of adaptation: motion adaptation. We used transparent motion as an adapting stimulus to trace the effects of adaptation through the motion processing hierarchy.

A transparent motion stimulus (Qian, Andersen, & Adelson, 1994a; Verstraten et al., 1994) contains multiple motion components¹ overlapping in the same spatial region. Numerous evidence shows that the processing of transparent motion involves multiple levels of motion analysis, including the extraction of local motion signals based on detectors with small receptive fields, such as V1 neurons, followed by a pooling of these local measurements through spatial integration based on detectors with large receptive fields, such as MT neurons (Qian & Andersen, 1994; Qian, Andersen, & Adelson, 1994a, 1994b; Snowden, Treue, Erickson, & Andersen, 1991). Transparent motion, thus, provides a useful tool to investigate how adaptation affects multiple stages within the motion processing hierarchy.

In addition, there is a puzzling perceptual effect in transparent motion adaptation. Although observers can simultaneously perceive multiple component motion

directions when adapting to transparent motion (Snowden & Verstraten, 1999), such adaptation generally elicits a unidirectional, integrated motion aftereffect (MAE) opposite to the average of the adapting directions (Mather, 1980; Snowden & Verstraten, 1999; Verstraten et al., 1994). This integrated MAE percept after adapting to bidirectional transparent pattern was first explained by the distribution-shift model (Mather, 1980). However, this model cannot explain why multiple directions in the transparent stimulus can be readily segmented and simultaneously perceived (Grunewald & Lankheet, 1996). Therefore, it remains unclear why motion segmentation is performed during transparent motion adaptation, yet such segmentation information does not influence the subsequent aftereffect to produce transparent MAE (Snowden & Verstraten, 1999).

Two competing theories have offered different explanations for why adaptation to multiple directions of motion yields a unidirectional, integrated MAE under most conditions. Grunewald and Lankheet (1996) proposed that transparent motion adaptation modulates the interactions between neurons tuned to different global motion directions. In this view, adaptation-induced changes primarily occur at the stage of global motion processing through a broadly tuned, inhibitory mechanism. In contrast, Vidnyanszky, Blaser, and Papathomas (2002) proposed that prolonged exposure to a transparent motion stimulus induces *bidirectional* local motion signals at each position and activates local mechanisms to average the different motion signals, resulting in unidirectional local aftereffects at each position. At the higher level, motion integration stage, these local aftereffects are integrated over space to generate the unidirectional MAEs. This theory, thus, supports the hypothesis that transparent motion adaptation involves an essential step of local aftereffect integration. Consistent with this local processing account, Curran, Clifford, and Benton (2006) used unidirectional random-dot kinematograms to show that the perceived directional aftereffect is mainly driven by the adaptation of motion-sensitive cells at the local processing stage of motion analysis. In addition, a recent study by Scarfe and Johnston (2011) provided compelling evidence that a unidirectional moving pattern can bias the perceived local aftereffects, suggesting that low-level detectors not only project motion signals to, but also receive feedback from, cells involved in high-level motion processing.

The present study aims to reconcile these two accounts for transparent motion adaptation within a coherent framework. We developed a novel experimental paradigm to show that adaptation to bidirectional transparent motion patterns can lead to two radically different types of MAEs: segregated and integrated MAEs. The segregated MAE yields an aftereffect opposite to one of the adapting directions in the transparent motion stimulus. In contrast, the integrated MAE yields an aftereffect opposite to the average of the adapting directions. [Experiment 1](#) shows that when local-level adaptation is strong, local adaptation

effects are propagated to higher level motion processing. The integration of these local aftereffects gives rise to the percept of a segregated MAE, which possibly overrides integrated MAE resulting from adaptation-induced modulation at the global level. [Experiments 2](#) and [3](#) show that, when local adaptation effects are eliminated or weakened, perceived MAE is dominated by the global-level adaptation effects, resulting in an integrated MAE.

Methods

Stimuli

We employed a multiple-aperture stimulus composed of multiple randomly oriented, drifting sinusoidal gratings (Amano, Edwards, Badcock, & Nishida, 2009; Clark & Bradley, 2008; Lee & Lu, 2010), as shown in [Figure 1A](#). Grating elements drifted within fixed windows to generate local motion signals, which could produce strong local adaptation effects after prolonged viewing. These illusory motion signals of local aftereffects show different motion directions and speeds because grating orientation was randomly assigned for each location. Drifting speed of each element was controlled to generate globally coherent motion through spatial integration. A transparent motion display can be constructed by randomly grouping the elements into two sets (as color-coded in [Figure 1](#)) and assigning two different global motion directions to the two sets, respectively. The resulting percept resembles those described in previous studies of transparent motion using random-dot kinematograms, in which two segregated motion directions can be perceived (Amano et al., 2009).

The multiple-aperture stimulus ([Figure 1A](#)) consisted of 396 drifting Gabor elements arranged in a circular pattern inscribed in a 24×24 grid, without any separation between each cell. Each Gabor element, subtending a visual angle of 1° , was constructed by imposing a stationary Gaussian function over an oriented sinusoidal grating, with spatial frequency being 2 cycles/deg and the standard deviation of the Gaussian window being 0.3° . Distance between the centers of two adjacent Gabors was 1° . The stimulus was displayed within an annulus spanning 4° – 12° around fixation. As population receptive field size of V1 in the human brain has been found to be under 1° within our stimulus range of eccentricity (Dumoulin & Wandell, 2008), integration of multiple elements by a local motion detector in V1, if any, should be minimal.

Orientation of each Gabor element was randomly assigned on each trial. For each Gabor element, the local drifting speed u was computed as follows:

$$u = v \sin(\alpha - \theta), \quad (1)$$

where α is the global motion direction, v is the global motion speed, and θ is the orientation assigned to the

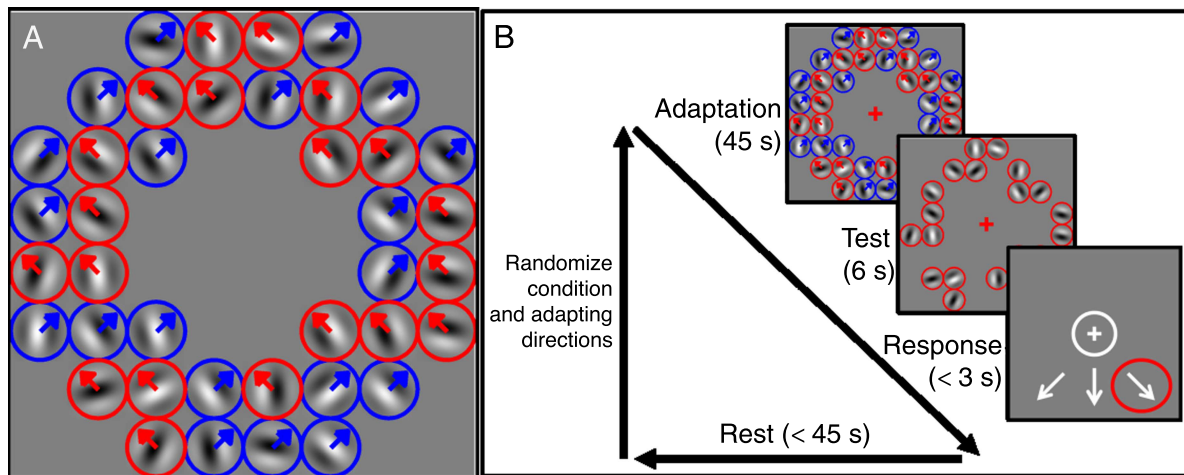


Figure 1. Illustrations of the stimulus and general procedure. (A) The adapting stimulus consisted of multiple drifting grating elements. Colors code the two Component Sets to which elements are randomly assigned (red: Set 1, blue: Set 2). The arrow overlaid on each element indicates the assigned global motion vector (up left for Set 1 and up right for Set 2). (B) Procedure for a sample trial (a *Single* condition). Colors and arrows on Gabor elements are for illustration only and were not presented during the experiments. Number of elements is reduced for the purpose of illustration.

element. This way of computing the local drifting speeds ensures that local motion vectors of all elements are consistent with the assigned global motion. Low contrast (0.05) for all Gabor elements was used to elicit strong spatial integration to facilitate the perception of global motion from the multiple-Gabor stimulus (Amano et al., 2009).

The transparent motion pattern

All transparent motion patterns in the present study contained two component motion directions. Each Gabor element was randomly assigned to one of two sets, and each set was assigned with component motion vector. As a result, the two component sets of elements were spatially separated with random configuration. Elements in Set 1 were assigned a global motion direction of $(X - 45)^\circ$, while elements in Set 2 were assigned $(X + 45)^\circ$, in which X° indicate the averaged or integrated direction of two component velocities. Eight integrated motion directions (from 0° to 315° , with 45° separation) were used in the experiments. Global motion speed was set at $v = 3.15^\circ/\text{s}$ for both component vectors.

This method of generating transparent motion pattern was adopted from the study by Amano et al. (2009). The main difference was that they employed a transparent motion stimulus with two component directions 180° apart (i.e., opposite), whereas ours were always 90° apart. Amano et al. showed that orientations of Gabor elements need to be randomized in order to perceive transparent motion. In a separate experiment, we verified that observers can reliably identify the two individual directions embedded in this stimulus. Eleven observers were instructed to report as many directions as they perceived

on the transparent pattern. They indicated their perceived directions, one after another, by turning a simulated dial on the computer screen. As shown in Figure 2, observers perceived two directions in the majority of trials. The reported perceived directions were found to peak at two directions, which generally coincide with the two directions embedded in the adapting stimulus. This finding justifies the use of this stimulus as a bidirectional, transparent motion pattern.

General procedure

Each trial consisted of three phases: adaptation (45 s), test (6 s), and response (<3 s; Figure 1B). First, during adaptation observers viewed the transparent motion pattern, with fixation maintained at the central cross. Then, they were presented with a static test pattern, with elements taken directly from the last frame of the adaptation motion sequence, while maintaining fixation at the central cross. Observers indicated their perceived motion direction of the aftereffect by choosing one of the following 4 options: 3 directional responses and 1 “no-motion” response, as illustrated in Figure 1B. Suppose a trial was assigned the integrated direction X° . Then, the adapting directions of Component Sets 1 and 2 were $(X - 45)^\circ$ and $(X + 45)^\circ$, respectively. The three directional response options were always $(X + 135)^\circ$, $(X - 135)^\circ$, and $(X - 180)^\circ$, which were opposite to Set 1, Set 2, and the integrated adapting directions, respectively. The first two responses were defined as segregated MAEs, while the third response was defined as integrated MAE.

There was a rest period of at least 45 s after each response. Each observer completed 8 trials for each condition in each experiment, with each trial corresponding to one of the

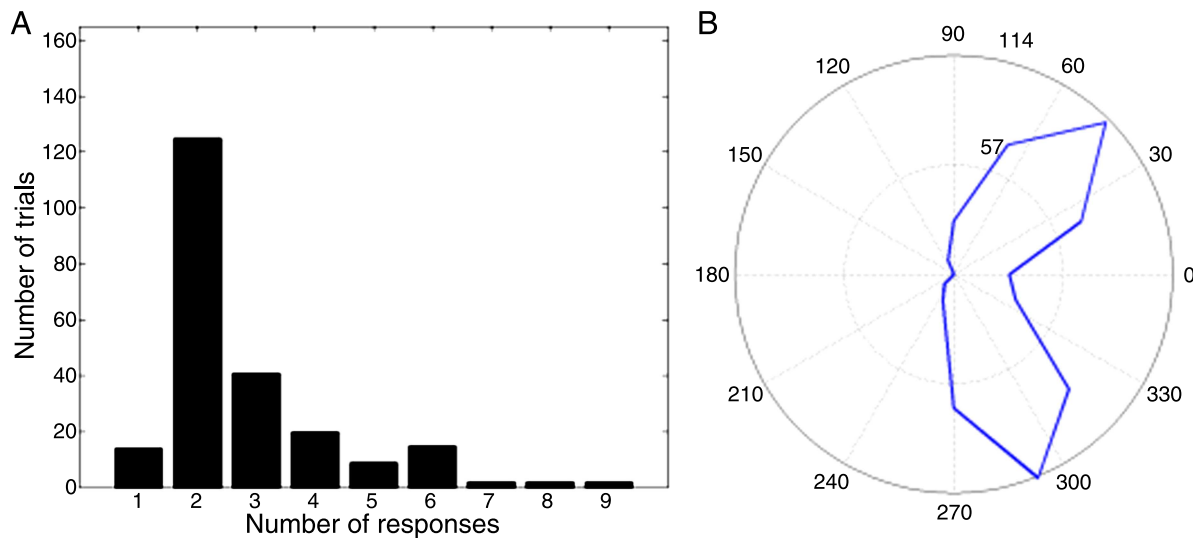


Figure 2. Distributions of perceived directions on the multiple-aperture transparent pattern in the dial-turning task. The stimulus contained two global directions that are 90° apart. (A) Distribution of numbers of responses across all observers (230 trials in total). (B) Distribution of perceived directions. Angles represent reported directions. Distance from center represents number of trials. Responses are aligned so that the two embedded directions in the stimulus are 45° and 315° (i.e., -45°).

8 integrated directions. Orders of conditions and directions were randomized for each subject.

Stimuli were generated using MATLAB and PsychToolbox (Brainard, 1997; Pelli, 1997) and presented on a Viewsonic CRT monitor with a refresh rate of 75 Hz and resolution of 1024×768 pixels, with a viewing distance of 57 cm kept constant using a chin rest and forehead rest. Undergraduate students at the University of California, Los Angeles (UCLA), all with normal or corrected-to-normal vision and naive to the experimental purpose, participated in the three experiments for course credit. The experiments were approved by UCLA's Office for Protection of Research Subjects.

Experiment 1: Comparing perceived MAE direction tested at different locations

Methods

Test locations were manipulated across three conditions. We first tested the MAE at all adapted locations (the *All* condition), as shown in Figure 3A (left panel of Test). We then constructed a critical condition (the *Single* condition), in which the test pattern consisted of elements taken from only one of the two component sets (Figure 3A, middle panel of Test; see Movie 1A for a demo). The third condition was the *Mixed* condition (Figure 3A, right panel of Test; see Movie 1B for a demo), in which a random half of the test elements from each set was included. This

manipulation of the *Mixed* condition served to match the test element density in the *Single* condition, so that the *Mixed* and *Single* conditions only differed in terms of test locations. Ten naive observers participated in Experiment 1 for course credit.

In the *Single* condition, the two segregated MAE responses were classified as *tested* or *untested* segregated MAEs using the following procedure. Suppose, in a *Single*-condition trial, test elements were chosen from Component Set 2 with adaptation direction being $(X + 45)^\circ$. We defined the MAE direction $(X - 135)^\circ$, opposite to the tested set's adapting direction, as the *tested* segregated MAE response and the other segregated MAE direction $(X + 135)^\circ$ as the *untested* segregated MAE. In order to provide a fair comparison between the *Single* condition and the *All* and *Mixed* conditions, in the latter two conditions, one of the two component sets was randomly chosen as the "tested set," so that a segregated MAE response could be assigned accordingly to be *tested* or *untested*.

Results

The distinction between *tested* and *untested* segregated MAE responses in the *All* and *Mixed* conditions is for illustration purpose only. In our statistical analyses, we summed over the proportions of the two segregated responses in order to have a more conservative comparison within each of the *All* and *Mixed* conditions. In both the *All* and *Mixed* conditions, the proportion of integrated MAE (*All*: 71.3%; *Mixed*: 77.5%) was much higher than the sum of the two segregated MAE response proportions (*All*: 16.3%, $F(1, 9) = 27.99$, $p < 0.001$; *Mixed*: 12.5%, $F(1, 9) = 76.69$, $p < 0.001$; Figure 3B). Crucially, the

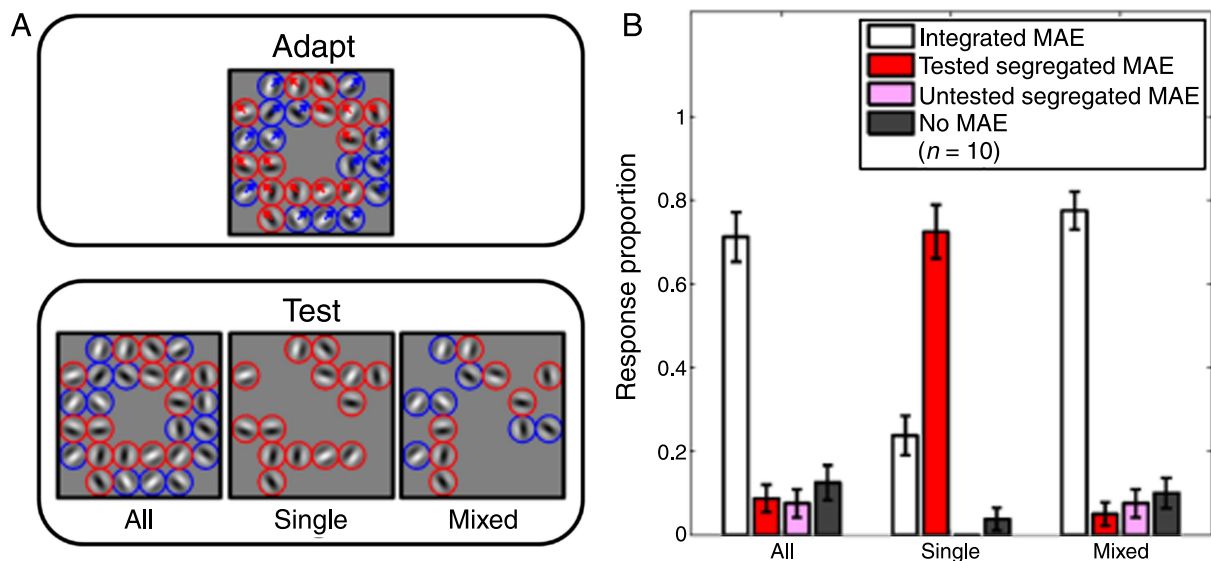
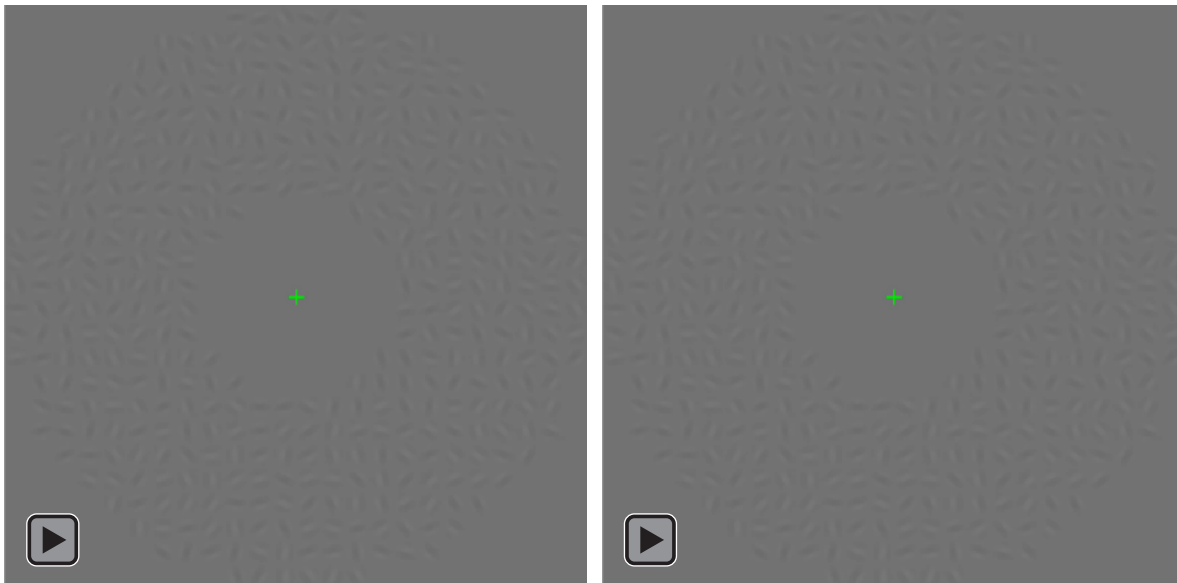


Figure 3. Conditions and results of Experiment 1. (A) Adapting stimulus was the same across conditions. Test conditions differed only in terms of where test elements were presented. (B) Proportions of reported MAE directions. Error bars are 1 SEM.

pattern was reversed in the *Single* condition: The proportion of tested segregated MAE responses (72.5%) was much higher than that of integrated MAE (23.8%, $F(1, 9) = 19.76$, $p = 0.002$). These results clearly demonstrate that when test elements are presented at locations of both component sets, an integrated MAE is found, with the aftereffect direction opposite to the average direction. However, when MAE was tested at the locations of only one component set (e.g., Set 1, adapting direction = $(X - 45)^\circ$), a segregated MAE was obtained, with the aftereffect direction opposite to the tested set's global adapting direction (e.g., MAE direction =

$(X + 135)^\circ$). Proportion of “no-motion” response was low across all conditions (means for *All* = 12.5%; *Single* = 3.8%; *Mixed* = 10.0%), indicating that relatively strong motion aftereffects were perceived by observers after transparent motion adaptation.

In order to confirm that observers perceived only one MAE direction on each trial, we reran the *Single* and *Mixed* conditions in Experiment 1 using a direction judgment task. Nine fresh observers were instructed to indicate as many directions as they had perceived during the test phase by turning a simulated dial on the screen. As shown in Figure 4A, the dominant response for the



Movie 1. Demonstrations for the *Single* (left) and *Mixed* (right) conditions in Experiment 1, respectively. Adaptation and test durations have been shortened to 30 s and 3 s, respectively, for illustration purpose. The two adapting directions are $+45^\circ$ and -45° (0° = upward, positive = clockwise) in both movies. In this demonstration the tested set's adapting direction is $+45^\circ$ for the *Single* condition (left).

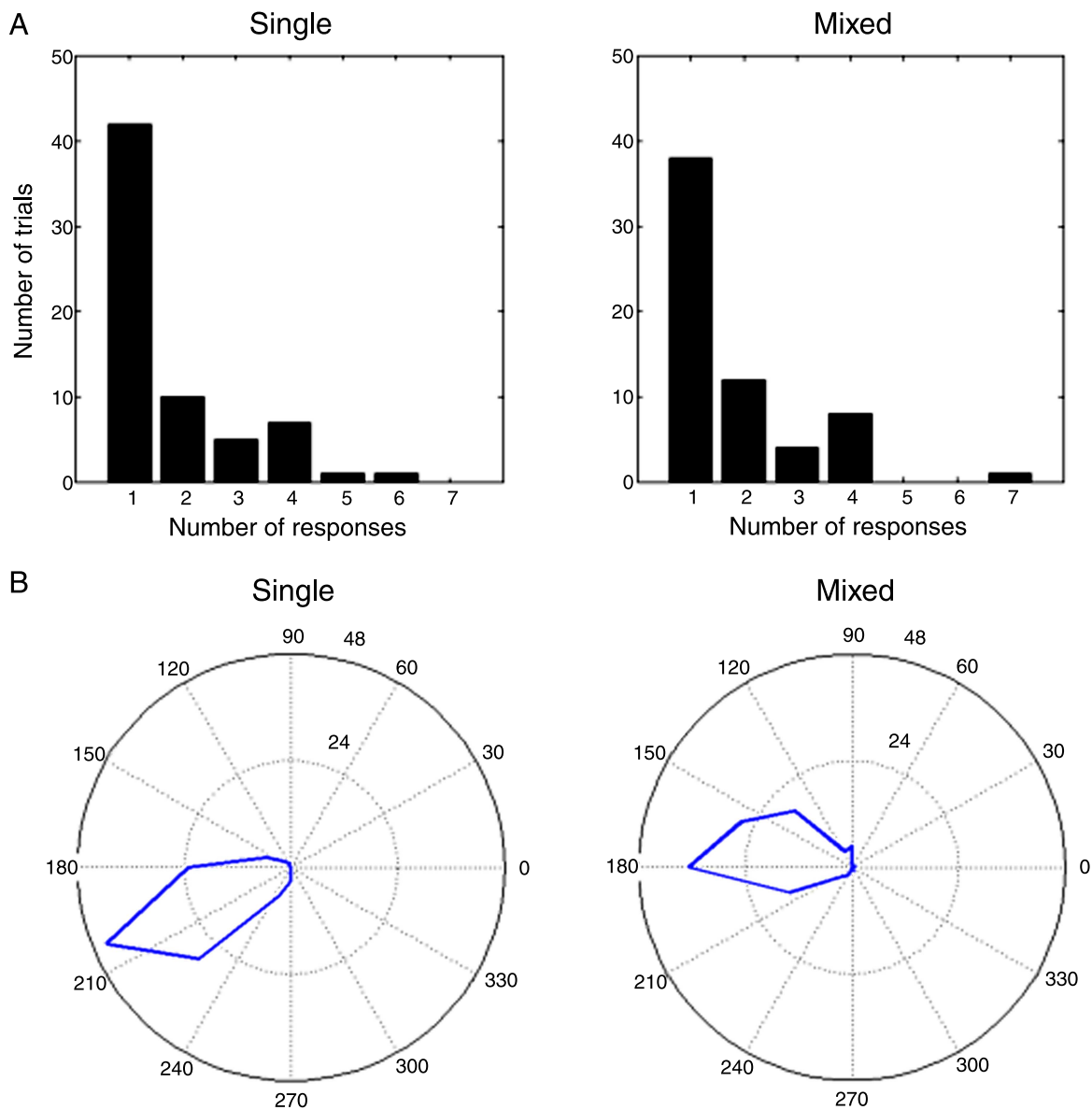


Figure 4. Distributions of perceived MAE directions in the dial-turning task for Experiment 1. (A) Histograms of the number of responses for the Single (left) and Mixed (right) conditions. (B) Distributions of perceived MAE directions for the Single (left) and Mixed (right) conditions. Angles represent reported directions. Distance from center represents number of trials. Responses are aligned so that the integrated direction (X°) in the adapting stimulus is at 0° . For the Single condition, responses are aligned so that the tested set's adapting direction is at 45° for every response.

number of perceived MAE directions was one direction in both the Single and Mixed conditions. In terms of perceived MAE directions (Figure 4B), results were similar to that found in the forced-choice task reported above, namely, observers primarily reported the tested segregated MAE direction (opposite to 45° in the figure) in the *Single* condition and the integrated MAE direction (opposite to 0° in the figure) in the *Mixed* condition.

Experiment 1 showed that, by manipulating testing locations, observers can be led to perceive either of two radically different forms of MAE after transparent motion adaptation. However, there are several possible ways in which adaptation could affect different motion processing

levels to elicit the two forms of aftereffects. One possible mechanism is that transparent motion adaptation alters response characteristics of global motion processors at MT, which integrates local motion information over the entire display window. As a result, adapting to two global motion directions ($X + 45^\circ$) and ($X - 45^\circ$) in a transparent motion display may change the tuning characteristics of MT cells that prefer the combined direction X° . This mechanism would lead to strong integrated MAE in the direction of ($X - 180^\circ$) but not location-specific segregated MAE. Another possibility is that the changes introduced at MT are due to the integration of local adaptation effects in early motion processing. This

mechanism would predict that perceived MAEs would be determined by the testing locations. However, this possibility hinges on the existence of local adaptation effects: If local aftereffects were eliminated, MAEs would not be observed. A third possibility is that both mechanisms exist in the motion system, as found in previous electrophysiological studies of contrast adaptation (Baccus & Meister, 2004; Kohn & Movshon, 2003; Solomon et al., 2004), and that they interact to produce motion aftereffects. [Experiments 2](#) and [3](#) aim to investigate which of the above possible mechanisms underlie the perceived aftereffect of transparent motion.

Experiment 2: Testing MAE at non-adapted locations

Methods

[Experiment 2](#) examined whether perceived MAEs depend on integration of local adaptation effects. Previous studies showed that motion aftereffects can be observed at non-adapted regions, a phenomenon termed “phantom” MAE (Snowden & Milne, 1997). The existence of phantom MAE provides evidence that adaptation induces changes at higher processing levels with larger receptive fields. Although test locations were fixed in [Experiment 2](#), these locations were either adapted or non-adapted in the

adaptation phase depending on different conditions ([Figure 5A](#)). Relative to the total number of elements (100%), 75% (37.5% from each of the two sets) were presented during the adaptation phase, leaving 25% (12.5% from each set) as non-adapted. Only 25% of elements were presented during the test phase, regardless of condition. In the *Adapted* condition, adapting elements from the *same* set were presented at test locations. As a result, the *Adapted* condition was identical to the *Single* condition of [Experiment 1](#), except that fewer elements were presented in both adaptation and test phases (see [Movie 2A](#) for a demo). In the *Non-adapted* condition, adapting elements were not presented at the test locations during the adapting phase in order to eliminate local adaptation effects. In other words, the test locations were empty during adaptation (see [Movie 2B](#) for a demo). [Experiment 2](#) aimed to examine the extent to which the segregated MAEs depend on the propagation of local adaptation effects in the early motion processing level. If the segregated MAE is largely due to integration of local adaptation effects, eliminating local motion adaptation would reduce the likelihood of perceiving segregated MAE. Thirteen naive observers participated in [Experiment 2](#) for course credits.

Results

[Figure 5B](#) shows that the tested segregated MAE (60.6%) was more frequently reported than the integrated MAE (22.1%) in the *Adapted* condition ($F(1, 12) = 12.63$,

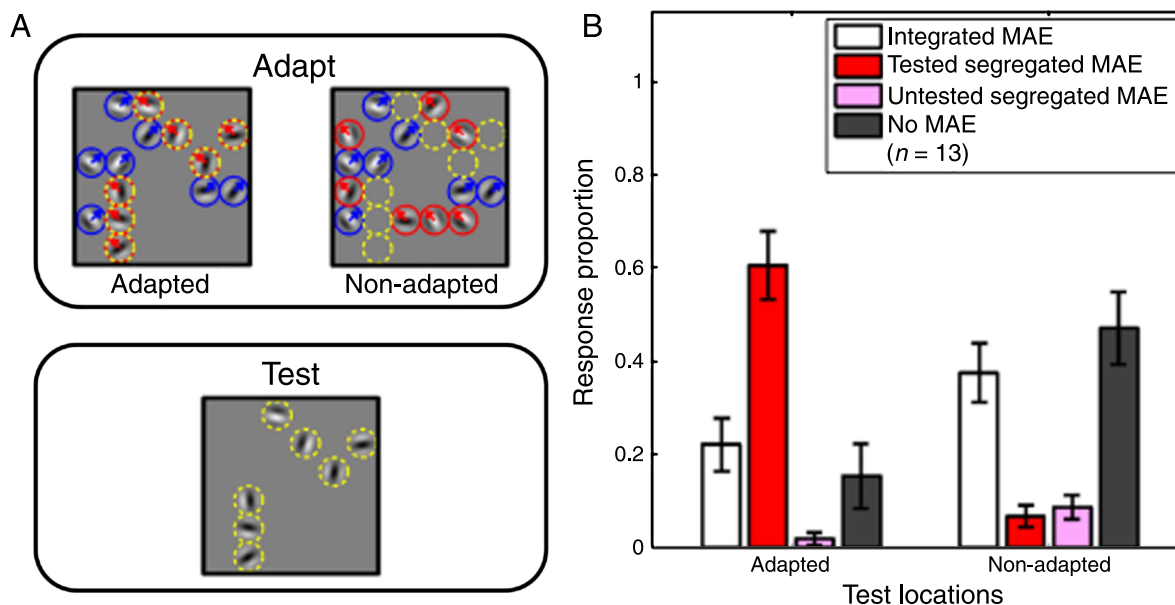
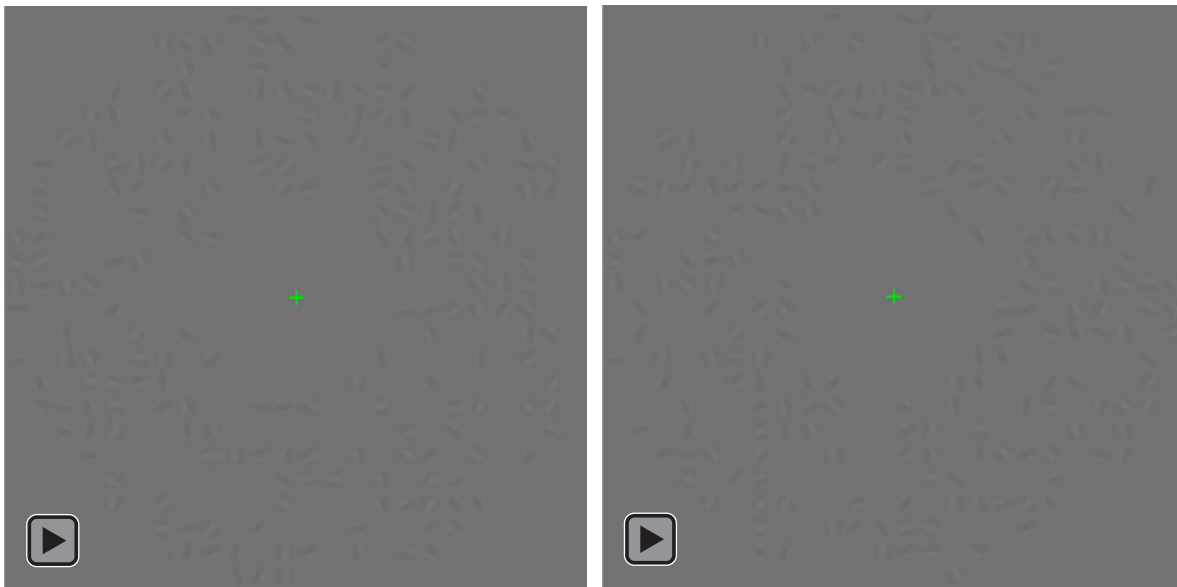


Figure 5. Conditions and results of [Experiment 2](#). (A) Unlike [Experiment 1](#), test locations were held constant (dashed yellow circles). The state of adaptation of these fixed test locations was manipulated. In the *Adapted* condition (top left), test locations overlap with adapting elements taken from one of the two component sets (dashed yellow on red, in this illustration). In the *Non-adapted* condition (top right), test locations (empty dashed yellow circles) did not overlap with any adapting elements. (B) Proportions of reported MAE directions. Error bars are 1 SEM.



Movie 2. Demonstrations for the *Adapted* (left) and *Non-adapted* (right) conditions in [Experiment 2](#), respectively. Stimulus parameters are similar to those in [Movies 1A](#) and [1B](#). In this demonstration the tested set's adapting direction is $+45^\circ$ for the *Adapted* condition (left).

$p < 0.01$; [Figure 5B](#), left group), replicating the findings of the *Single* condition in [Experiment 1](#). The negligible proportion of untested segregated MAE (1.9%) could be due to response noise (as it was not observed in [Experiment 1](#)) and was not considered in the analysis. In contrast, when tested at non-adapted locations ([Figure 5B](#), right group), observers still perceived an MAE, but this “phantom” MAE was found to be dominated by the integrated direction (37.5%) as the proportion of segregated MAE responses (15.4%) was smaller ($F(1, 12) = 10.11, p < 0.01$). As we switched from the *Adapted* to the *Non-adapted* conditions by eliminating the effects of location adaptation, the proportion of segregated MAE responses greatly reduced from 60.6% to 15.4% ($F(1, 12) = 41.55, p < 0.001$). This significant reduction in segregated MAE clearly supports the hypothesis that the segregated MAE mainly results from the integration of local adaptation effects. A significant two-way interaction (MAEs \times Conditions: $F(1, 12) = 25.86, p < 0.001$) further demonstrates that the elimination of local adaptation shifted the perceived aftereffect direction from segregated MAE to integrated MAE.

Note that the perceived aftereffect in the *Non-adapted* condition was relatively weak. The proportion of “no-MAE” responses was 47.1%, meaning that observers reported perceiving an MAE in only 52.9% of trials (cf. “no-MAE” proportion in *Adapted*: 15.4%, MAE proportion: 85.6%). The weaker strength of aftereffect at non-adapted locations is consistent with other findings concerning phantom motion aftereffects (Snowden & Milne, 1997). In addition, observers in our experiment were naive undergraduate students who participated for course credits. It is likely that the inexperience of subjects also

contributed to the weak effect of adaptation. Nonetheless, our results indicate that observers consistently reported integrated MAE when they perceived an aftereffect in a trial in the *Non-adapted* condition. In order to find out whether observers reported integrated MAE more frequently than chance level, we computed the normalized proportion for the integrated MAE responses. For each condition, we divided the integrated MAE response proportion by the total proportion of MAE responses. For a more conservative test, we compared this value with the chance-level performance in a 2AFC task (50%), as if observers were to choose between the integrated and segregated MAE directions. We found that the integrated MAE was perceived more frequently than chance in the non-adapted regions² (normalized proportion of integrated MAE responses = 73.0%; $t(11) = 3.40, p = 0.006$). This indicates that, to some extent, adaptation at higher processing levels contributes to the perceived phantom MAE in non-adapted locations.

This manipulation in our [Experiment 2](#) is similar to that used in a recent study by Scarfe and Johnston (2011). The key difference is that we used transparent motion as the adapting stimulus, whereas Scarfe and Johnston used unidirectional moving Gabor arrays as the adapting stimulus in their Experiment 3. Participants in their experiment reported “no MAE” on more than 90% of trials, indicating the absence of phantom MAE. One possible account for the discrepancy between the two studies could be due to eye movements. Since we used inexperienced observers who may have poor ability to maintain a steady fixation during adaptation, eye movements may play essential role in revealing the phantom MAE found in our study.

We assessed this possibility with a follow-up experiment using similar procedure as the *Non-adapted* condition in [Experiment 2](#) but employed a different adaptation stimulus and a different task. Instead of two translational 2D vectors assigned to the two component sets of elements, global motion for each set was a spiral (radial + rotational). Elements in one set were assigned 2D velocities that were consistent with a global clockwise-inward (or outward, radial directions randomized across trials) spiral, which is analogous to the $(X + 45)^\circ$ direction in the original experiments. Elements in the other set were assigned a counterclockwise-inward (or outward) spiral, which is analogous to the $(X - 45)^\circ$ direction. This stimulus was perceived to be an overall radial motion, with a certain level of rotational transparency. After adapting to this stimulus, observers were presented with the static test stimulus, with all elements shown at non-adapted locations (same as the *Non-adapted* condition in [Experiment 2](#)). During the response phase, observers first indicated whether they saw an MAE or not. If they indicated that they saw an MAE, they were then asked to indicate the direction of the perceived MAE in a 3AFC task, with the 3 alternatives being clockwise-outward spiral, purely outward, and counterclockwise-outward spiral (for outward adapting stimuli, radial direction in all alternatives was “inward”). If they reported “no MAE,” the trial ended at that point. Four experienced observers (at least 3 years of experience in visual psychophysics), who knew neither the purpose nor the design of the experiment, participated. Each observer completed 16 trials.

Results from individual observers are shown in [Figure 6](#). All 4 observers consistently reported seeing the phantom MAE above chance level, except that JS reported the phantom MAE in 10 out of 16 trials, slightly above chance ([Figure 6A](#)). To assess how frequently each MAE

direction observers perceived, we computed the normalized response proportion for each MAE direction. The proportions were “normalized” against the total number of trials in which MAE was perceived (e.g., if JS perceived a purely radial MAE in 8 trials out of the 10 trials in which she saw an MAE, the normalized proportion for “radial” would be 80%). There is a consistent trend across observers ([Figure 6B](#)): The dominant perceived direction of the phantom MAE was in the radial direction, which is analogous to the dominant “integrated” direction in the phantom MAE described in [Experiment 2](#).

Results from the follow-up experiment are consistent with those in [Experiment 2](#), providing further evidence for the existence of an integrated, phantom MAE after adapting to transparent motion generated from a multiple-aperture stimulus. The results also show that it is unlikely that the phantom MAE can be explained largely by eye movements. This finding is inconsistent with those reported by Scarfe and Johnston (2011). We suspect that this discrepancy is mainly due to the difference in adaptation durations. In their study, adaptation lasted for 8 s on the first trial, with 3-s top-ups. An 8-s adaptation is much shorter than the durations used in previous phantom MAE studies, in which adaptation duration ranged from 30 to 120 s, with top-ups of 4 to 5 s (Price, Greenwood, & Ibbotson, 2004; Snowden & Milne, 1997; Weisstein, Maguire, & Berbaum, 1977). In our experiments, adaptation lasted for 45 s on all trials, which is within the range of adaptation duration used in previous studies in which phantom MAE was observed. It has also been shown that the strength of MAE positively correlated with adaptation duration (Hershenson, 1993). Another potential reason for the discrepancy may involve contrasts. Our stimulus employed low contrast (0.05) for both adapting and testing stimuli, whereas Scarfe and Johnston used 0.3

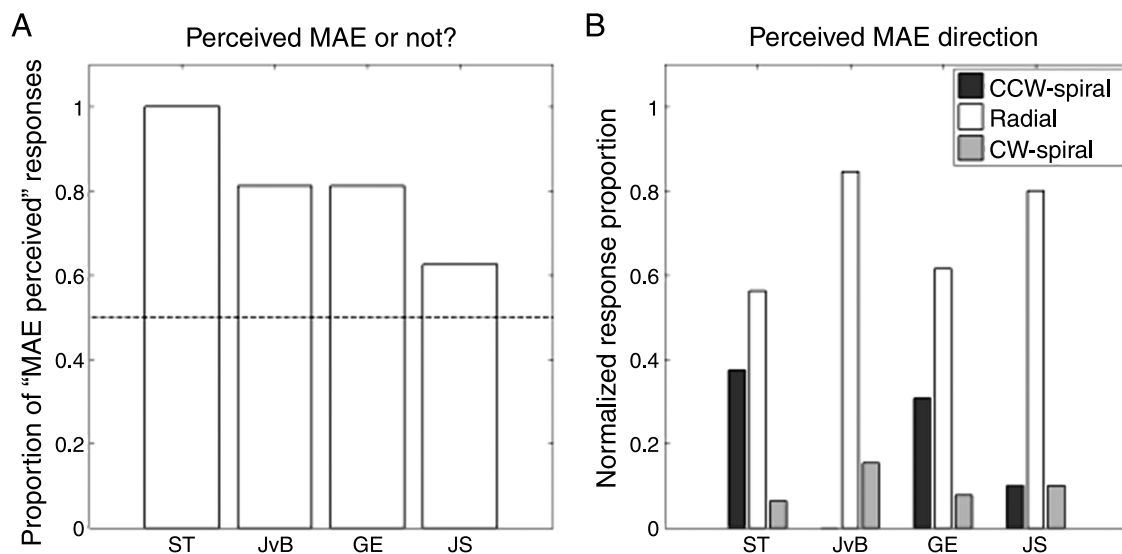


Figure 6. Results of individual experienced observers on complex phantom MAE. (A) Proportion of trials in which observers indicated that they saw MAE. (B) Response proportions for each directional response, normalized within trials in which MAE was perceived.

contrast for adapting and 0.8 for testing stimuli. As suggested by Amano et al. (2009), high stimulus contrasts may impair spatial integration, which could weaken the percept of global motion generated from a multiple-Gabor stimulus. We conjecture that low contrasts may also strengthen motion integration and interpolation after adaptation, which in turn increases the possibility of perceiving the illusory phantom MAE.

Experiment 3: Testing MAE at non-adapted orientations

Methods

Experiment 3 varied the strength of local adaptation effects by exploiting the property that local motion processors in V1 are orientation-selective. Previous studies (Hammond, Pomfrett, & Ahmed, 1989; McGraw, Whitaker, Skillen, & Chung, 2002) have shown that motion aftereffects are substantially reduced when the test grating has an orientation orthogonal to that of the adapting grating. We therefore manipulated the orientations of test elements, either keeping them the same as adapting elements or rotating them by 90° from adapting orientations. As in **Experiment 1**, we included testing locations as an independent variable. Accordingly, this design involved four experimental conditions (**Figure 7A**): *Mixed*, *Orthogonal-Mixed*, *Single*, and *Orthogonal-Single*, which allows us to examine how local adaptation effects interact with integrated MAE. Nineteen naive observers participated in **Experiment 3** for course credit.

Results

As shown in **Figure 7B**, when test elements are presented at locations of both adapting sets (the two *Mixed* conditions), integrated MAE was more frequently reported than segregated MAEs in both conditions (*Mixed*: Integrated (59.9%) vs. sum of segregated (19.1%), $F(1, 18) = 34.46$, $p < 0.001$; *Ortho-Mixed*: Integrated (43.4%) vs. sum of segregated (19.7%), $F(1, 18) = 11.83$, $p < 0.005$). However, this dominant integrated MAE was weakened when test orientations were made orthogonal to adaptation orientations. The proportion of integrated MAE in the *Orthogonal-Mixed* condition (43.4%) was lower than that in the *Mixed* condition (59.9%), $F(1, 18) = 5.580$, $p < 0.05$. This finding indicates that integration of local adaptation effects may contribute to the integrated MAE. When test locations were chosen from only one adapting set (the two *Single* conditions), a dominant tested segregated MAE (58.6%) was obtained when identical

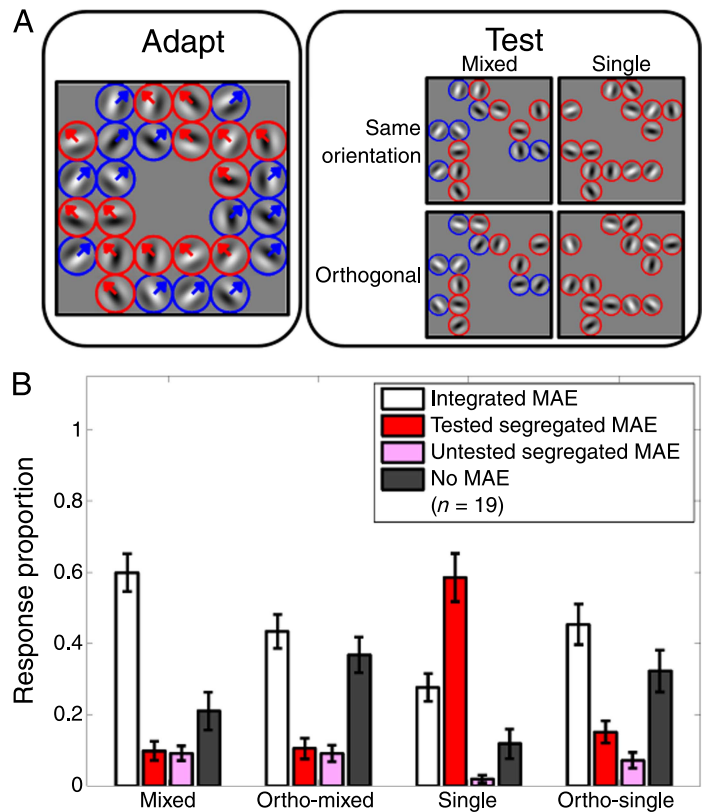


Figure 7. Conditions and results of **Experiment 3**. (A) Procedure and conditions were the same as in **Experiment 1**, except for the introduction of test orientation as an independent variable, resulting in 4 conditions. (B) Proportions of reported MAE directions. Error bars are 1 SEM.

orientations were used for adapting and testing stimuli (*Single*: tested segregated (58.6%) vs. integrated MAE (27.6%), $F(1, 18) = 9.48$, $p < 0.01$), replicating the results in **Experiment 1**. As in **Experiment 2**, the negligible proportion of untested segregated MAE responses, 2.0%, was not included in the analysis. However, when orthogonal orientations were tested in the *Orthogonal-Single* condition, perceived MAE was biased more toward the integrated (45.4%) than the segregated directions (tested = 15.1%; untested = 7.2%). Specifically, the proportion of integrated MAE responses was larger than the sum of the two segregated MAE response proportions ($F(1, 18) = 9.32$, $p < 0.01$). A significant simple two-way interaction between test orientation and perceived MAE direction for the two *Single* conditions ($F(1, 18) = 18.62$, $p < 0.001$) provides further evidence that the integration of local adaptation effects was the major mechanism contributing to the perceived segregated MAE. In addition, there were generally more “no-motion” responses in the orthogonal conditions (*Orthogonal-Mixed* = 36.8%; *Orthogonal-Single* = 32.2%) than in the same-orientation conditions (*Mixed* = 21.1%; *Single* = 11.8%; $F(1, 18) =$

11.03, $p < 0.005$), confirming that the use of orthogonal test orientations effectively weakened the strength of perceived motion aftereffects.

General discussion

The present study shows that adaptation to bidirectional transparent motion can induce two radically different motion aftereffects and elucidates the linkage between these perceptual aftereffects and different motion adaptation mechanisms in the visual system. [Experiment 1](#) shows that test locations determine which form of MAE observers perceive after adapting to transparent motion. When the test stimulus contained elements chosen from only one of the two component sets, perceived MAE direction was found to be opposite to adapting direction of the chosen set (a *tested segregated MAE*). When the test stimulus contained elements randomly chosen from both sets, perceived MAE direction was opposite to the average of the two adapting directions (an *integrated MAE*). [Experiment 2](#) investigated the mechanisms underlying the two forms of MAE. We found that, when local adaptation was eliminated, segregated MAE diminished and integrated MAE reemerged. This finding suggests that the segregated MAE results from integration of local motion aftereffects via the propagation of adaptation-induced changes in early processing areas (i.e., V1), and part of the integrated MAE is due to global motion adaptation via directly modulating responses of neurons at the global processing stage (i.e., MT). [Experiment 3](#) shows that integration of local motion aftereffects, as a second source of adaptation-induced changes, also plays a role in determining the magnitude of integrated MAE perceived by the observers.

The multiple-aperture adapting stimulus used in our experiments is able to yield the percept of bidirectional motion transparency. Amano et al. (2009) reported that, when Gabor elements in the same component set were assigned the same orientation, the “transparent” pattern was perceived to be unidirectional. However, by randomizing the orientations of elements within each component set, we increased the variability in local drifting velocities and, thus, reduced the coherence across the two sets. This made the two individual directions of the components more salient. As shown in the results reported of our preliminary experiment, observers simultaneously perceived the two global directions when presented with our adapting stimulus, instead of perceiving the unidirectional, integrated one.

Our general findings are consistent with those reported by Scarfe and Johnston (2011). Both studies indicate that the visual system enables the integration of ambiguous local motion signals to infer global motion and, meanwhile, retains local spatial precision that is important

for representing motion boundaries and features (Braddick, 1993). These findings are consistent with a line of research on the importance of local adaptation in generating an MAE percept (Curran et al., 2006; Lopez-Moliner, Smeets, & Brenner, 2004; Vidnyanszky et al., 2002). However, a significant discrepancy between the two studies concerns findings of phantom MAEs using multiple-aperture stimulus. We found evidence of a weak phantom MAE at non-adapted locations after adapting to transparent motion, whereas Scarfe and Johnson’s study did not reveal any phantom MAE after adapting to unidirectional motion. We conjecture that this difference may be largely due to adaptation duration and stimulus parameters, such as contrasts.

Our results show that transparent motion adaptation induces changes at both local and global levels of motion processing. Two different neural adaptation mechanisms are involved: integration of adaptation effects at the local processing level and adaptation-induced modulation at the global level. The hypothesis that the visual system utilizes a combination of these two mechanisms can explain why most previous studies on transparent motion adaptation found an integrated MAE but not a segregated MAE, which was found in our *Single* conditions. A multiple-aperture stimulus enhances the possibility of finding the two forms of aftereffects, mainly due to orientation selectivity of local motion detectors in V1. Random-dot (Alais, Verstraten, & Burr, 2005; van der Smagt, Verstraten, & van de Grind, 1999) or random-pixel (Verstraten et al., 1994) patterns contain a distribution of orientations at each location and stimulate detectors preferring a range of orientations within one location. Therefore, it is challenging to design a test stimulus for these adapting patterns to examine the specific local aftereffects generated by orientation-selective local motion detectors. In contrast, the multiple-aperture stimulus specifically stimulates local motion detectors at one orientation at each location. This stimulus makes it possible to design a test stimulus such that effects of adaptation at those adapted orientations (or non-adapted orientations, as in [Experiment 3](#)) can be measured. Such differences in the potential to extract local MAEs between types of stimuli explain why most previous studies did not find the segregated MAE.

In the psychophysics literature, the segregated MAE has never been observed after transparent motion adaptation, unless other cues distinguish the two component motion patterns, such as speed (van der Smagt et al., 1999; Verstraten, van der Smagt, Fredericksen, & van de Grind, 1999), temporal frequency (Alais et al., 2005), or binocular disparity (Curran, Hibbard, & Johnston, 2007; Verstraten, Verlinde, Fredericksen, & Vandegrind, 1994). However, the segregated MAEs observed in these previous studies could possibly result from two different neural adaptation mechanisms. (1) Adaptation may induce changes at a low-level processing stage, and then local aftereffects associated with the same cue value may be

integrated to produce the perceived segregated MAE. (2) Adaptation may induce changes in different tuning channels (e.g., speed-tuned channels in MT) at the global motion processing level. Accordingly, the paradigms used in these previous studies could not clarify which adaptation mechanism the visual system adopts. In our study, spatial separation allows us to probe the adaptation to each component motion after adapting to a transparent motion stimulus. Although spatial separation of component motions accomplishes practically the same function as assigning different speeds to two component motions, there are no tuning channels at the global motion processing level corresponding to different spatial separations. The segregated MAEs revealed in our study thus provide direct evidence of the integration of local adaptation effects and the mechanisms of multilevel adaptation.

Our results show that adaptation is a complicated process, and an observed aftereffect is not necessarily generated from one single neural site. With an adapting stimulus that stimulates multiple levels of processing, observed aftereffects could result from neural changes at one level, propagated effects from lower to higher levels, and/or a combination of the two. Future research on sensory adaptation should focus on how to tease apart the contributions of multiple possible mechanisms for adaptation-induced changes in neural processing and perception.

Acknowledgments

This research was supported by a grant from the National Science Foundation (NSF BCS-0843880) and a UCLA Faculty Research Grant. We thank Jeroen van Boxtel for helpful discussion and Kimson Nguyen for his help in data collection.

Commercial relationships: none.

Corresponding author: Alan L. F. Lee.

Email: alanlee@ucla.edu.

Address: Department of Psychology, University of California, Franz Hall, Box 951563, Los Angeles, CA 90095-1563, USA.

Footnotes

¹The word “component” may lead readers to think of the “component vs. pattern” terminology used in the motion processing literature. To avoid confusion, the word “component” in this paper is used solely for referring to one of the multiple motion directions embedded in a transparent motion display and does *not* refer to the local drifting motion of gratings.

²One observer reported “no motion” in all trials of the *Non-adapted* condition. It is not possible to compute a normalized integrated MAE response proportion for this observer. Although this observer was included in the main analysis, he/she was not included in the test of “normalized proportion vs. chance”).

References

- Alais, D., Verstraten, F. A., & Burr, D. C. (2005). The motion aftereffect of transparent motion: Two temporal channels account for perceived direction. *Vision Research*, *45*, 403–412. [PubMed]
- Amano, K., Edwards, M., Badcock, D. R., & Nishida, S. (2009). Adaptive pooling of visual motion signals by the human visual system revealed with a novel multi-element stimulus. *Journal of Vision*, *9*(3):4, 1–25, <http://www.journalofvision.org/content/9/3/4>, doi:10.1167/9.3.4. [PubMed] [Article]
- Baccus, S. A., & Meister, M. (2004). Retina versus cortex: Contrast adaptation in parallel visual pathways. *Neuron*, *42*, 5–7. [PubMed]
- Braddick, O. (1993). Segmentation versus integration in visual-motion processing. *Trends in Neurosciences*, *16*, 263–268. [PubMed]
- Brainard, D. H. (1997). The psychophysics toolbox. *Spatial Vision*, *10*, 433–436. [PubMed]
- Clark, A. M., & Bradley, D. C. (2008). *Integration of distributed one-dimensional motion signals by macaque middle temporal cortical neurons*. Paper presented at the Computational and Systems Neuroscience (Cosyne), Salt Lake City, UT. [Abstract]
- Clifford, C. W., Webster, M. A., Stanley, G. B., Stocker, A. A., Kohn, A., Sharpee, T. O., et al. (2007). Visual adaptation: Neural, psychological and computational aspects. *Vision Research*, *47*, 3125–3131. [PubMed]
- Curran, W., Clifford, C. W. G., & Benton, C. P. (2006). The direction aftereffect is driven by adaptation of local motion detectors. *Vision Research*, *46*, 4270–4278. [PubMed]
- Curran, W., Hibbard, P. B., & Johnston, A. (2007). The visual processing of motion-defined transparency. *Proceedings of the Royal Society of London B: Biological Sciences*, *274*, 1049–1056. [PubMed] [Article]
- Dragoi, V., Sharma, J., & Sur, M. (2000). Adaptation-induced plasticity of orientation tuning in adult visual cortex. *Neuron*, *28*, 287–298. [PubMed]
- Dumoulin, S. O., & Wandell, B. A. (2008). Population receptive field estimates in human visual cortex. *Neuroimage*, *39*, 647–660. [PubMed] [Article]

- Grunewald, A., & Lankheet, M. J. (1996). Orthogonal motion after-effect illusion predicted by a model of cortical motion processing. *Nature*, *384*, 358–360. [PubMed] [Article]
- Hammond, P., Pomfrett, C. J., & Ahmed, B. (1989). Neural motion after-effects in the cat's striate cortex: Orientation selectivity. *Vision Research*, *29*, 1671–1683. [PubMed]
- Hershenson, M. (1993). Linear and rotation motion after-effects as a function of inspection duration. *Vision Research*, *33*, 1913–1919. [PubMed]
- Kohn, A., & Movshon, J. A. (2003). Neuronal adaptation to visual motion in area MT of the macaque. *Neuron*, *39*, 681–691. [PubMed]
- Kohn, A., & Movshon, J. A. (2004). Adaptation changes the direction tuning of macaque MT neurons. *Nature Neuroscience*, *7*, 764–772. [PubMed]
- Krekelberg, B., van Wezel, R. J. A., & Albright, T. D. (2006). Adaptation in macaque MT reduces perceived speed and improves speed discrimination. *Journal of Neurophysiology*, *95*, 255–270. [PubMed] [Article]
- Lee, A. L. F., & Lu, H. (2010). A comparison of global motion perception using a multiple-aperture stimulus. *Journal of Vision*, *10*(4):9, 1–16, <http://www.journalofvision.org/content/10/4/9>, doi:10.1167/10.4.9. [PubMed] [Article]
- Lopez-Moliner, J., Smeets, J. B. J., & Brenner, E. (2004). Components of motion perception revealed: Two different after-effects from a single moving object. *Vision Research*, *44*, 2545–2549. [PubMed]
- Mather, G. (1980). The movement aftereffect and a distribution-shift model for coding the direction of visual movement. *Perception*, *9*, 379–392. [PubMed]
- McGraw, P. V., Whitaker, D., Skillen, J., & Chung, S. T. (2002). Motion adaptation distorts perceived visual position. *Current Biology*, *12*, 2042–2047. [PubMed]
- Pelli, D. G. (1997). The VideoToolbox software for visual psychophysics: Transforming numbers into movies. *Spatial Vision*, *10*, 437–442. [PubMed]
- Price, N. S. C., Greenwood, J. A., & Ibbotson, M. R. (2004). Tuning properties of radial phantom motion aftereffects. *Vision Research*, *44*, 1971–1979. [PubMed]
- Qian, N., & Andersen, R. A. (1994). Transparent motion perception as detection of unbalanced motion signals: 2. Physiology. *Journal of Neuroscience*, *14*, 7367–7380. [PubMed] [Article]
- Qian, N., Andersen, R. A., & Adelson, E. H. (1994a). Transparent motion perception as detection of unbalanced motion signals: 1. Psychophysics. *Journal of Neuroscience*, *14*, 7357–7366. [PubMed] [Article]
- Qian, N., Andersen, R. A., & Adelson, E. H. (1994b). Transparent motion perception as detection of unbalanced motion signals: 3. Modeling. *Journal of Neuroscience*, *14*, 7381–7392. [PubMed] [Article]
- Scarfe, P., & Johnston, A. (2011). Global motion coherence can influence the representation of ambiguous local motion. *Journal of Vision*, *11*(12):6, 1–11, <http://www.journalofvision.org/content/11/12/6>, doi:10.1167/11.12.6. [PubMed] [Article]
- Schrater, P. R., & Simoncelli, E. P. (1998). Local velocity representation: Evidence from motion adaptation. *Vision Research*, *38*, 3899–3912. [PubMed]
- Snowden, R. J., & Milne, A. B. (1997). Phantom motion aftereffects—Evidence of detectors for the analysis of optic flow. *Current Biology*, *7*, 717–722. [PubMed]
- Snowden, R. J., Treue, S., Erickson, R. G., & Andersen, R. A. (1991). The response of area Mt and V1 neurons to transparent motion. *Journal of Neuroscience*, *11*, 2768–2785. [PubMed] [Article]
- Snowden, R. J., & Verstraten, F. A. (1999). Motion transparency: Making models of motion perception transparent. *Trends in Cognitive Sciences*, *3*, 369–377. [PubMed]
- Solomon, S. G., Peirce, J. W., Dhruv, N. T., & Lennie, P. (2004). Profound contrast adaptation early in the visual pathway. *Neuron*, *42*, 155–162. [PubMed]
- van der Smagt, M. J., Verstraten, F. A., & van de Grind, W. A. (1999). A new transparent motion aftereffect. *Nature Neuroscience*, *2*, 595–596. [PubMed]
- Verstraten, F. A., Fredericksen, R. E., & van de Grind, W. A. (1994). Movement aftereffect of bi-vectorial transparent motion. *Vision Research*, *34*, 349–358. [PubMed]
- Verstraten, F. A., van der Smagt, M. J., Fredericksen, R. E., & van de Grind, W. A. (1999). Integration after adaptation to transparent motion: Static and dynamic test patterns result in different aftereffect directions. *Vision Research*, *39*, 803–810. [PubMed]
- Verstraten, F. A. J., Verlinde, R., Fredericksen, R. E., & Vandegrind, W. A. (1994). A transparent motion aftereffect contingent on binocular disparity. *Perception*, *23*, 1181–1188. [PubMed]
- Vidnyanszky, Z., Blaser, E., & Pappathomas, T. V. (2002). Motion integration during motion aftereffects. *Trends in Cognitive Sciences*, *6*, 157–161. [PubMed]
- Weisstein, N., Maguire, W., & Berbaum, K. (1977). Phantom-motion aftereffect. *Science*, *198*, 955–958. [PubMed]